Available online at www.sciencedirect.com

ScienceDirect

Procedia Engineering 65 (2013) 311 – 320

Procedia Engineering

www.elsevier.com/locate/procedia

Concrete and Concrete Structures 2013 Conference

Influence of Corrosion on Crack Width and Pattern in an RC Beam

Peter Koteš[a,*]

[a]*University of Žilina, Civil Engineering Faculty, Univerzitná 8215/1, Žilina 010 26, Slovakia*

Abstract

The paper is concerned with numerical modeling of corrosion of steel reinforcement in the reinforced concrete. The cracking response of the reinforced concrete beams due to the corrosion effect of the steel reinforcement and due to the load effects was analyzed. The effect of corrosion was simulated by the nonlinear numerical analysis with the FEM program using the 3D model.

Selection and peer-review under responsibility of University of Zilina, Faculty of Civil Engineering, Department of Structures and Bridges

Keywords: Corrosion; existing bridges; crack; crack width; crack pattern; concrete cover; reinforcement;

1. Introduction

The concrete provides reliable protection of reinforcement, but the serious defects may occur. For example, it may be poor choice of concrete component, failures in building construction, unexpected effects of an action, as well as an increase in aggressiveness of environment. Thus with regards to serviceability, the condition of reinforcement and concrete quality are limiting factors for the resistance.

Safety, serviceability and durability are the basic parameters, which ensure the reliability of the construction as a whole or its parts [1]. The durability is the important parameter for design or evaluation of structures. The requirement to design durable structures means that the structure is not disturbed to an impermissible degree what would cause the limited serviceability due to the degradation processes during the planned design lifetime, provided that the maintenance and repairs are adequate. The durability ranks lower to both ultimate and serviceability limit states in terms of reliability. So, the durability is not verified, but is provided by design requirements.

* Tel.: +421-41-513-5663; fax: +421-41-513-5690.
E-mail address: kotes@fstav.uniza.sk

Selection and peer-review under responsibility of University of Zilina, Faculty of Civil Engineering, Department of Structures and Bridges
doi:10.1016/j.proeng.2013.09.048

The protection of reinforced concrete structures against corrosion is provided by design principles such as concrete cover and quality of concrete. The corrosion has a great effect on structure in terms of the ultimate limit state and serviceability limit state. Thus, the corrosion not only decreases the reinforcement cross-section area, thus decreasing the resistance as well, but it also increases the volume of the corrosive products (rust), giving rise to tensile and compressive stresses and then ultimately cracks, which are undesirable in terms of serviceability [2-4].

The paper deals with numerical 3D modeling of reinforcement corrosion in program Atena, which is used to verify the laboratory tests. The aim was to find out how the reinforcement corrosion affects the initiation and propagation of cracks in reinforced concrete with a focus on the crack width.

2. Experimental measurements on specimens

The numerical modeling is based on experimental measurements carried out at VUT Brno [5]. Forty samples of small beams with smooth-faced reinforcement class 10 216 and ten samples of small beams with tubular cross-section class 11 333 were made for diagnostic survey. The diameter of both bars (smooth-faced reinforcement and tube) was 6 mm (Fig. 1).

The maximum measured crack width was 0.60 mm in the case of beams with reinforcement class 10 216 and 0.65 mm in the case of tube class 11 333.

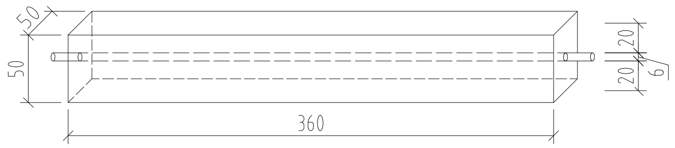

Fig. 1. Experimental specimen – small beams with dimensions.

The values from experiment shown in Fig. 2 are the average values from measurements. The corrosive environments were created during the experiment in order to accelerate the process of corrosive activity. Five percent aqueous solution of NaCL was used to create the appropriate corrosion conditions. The specimens were inserted into it only to 2/3 of their height for 16 hours and subsequently for 8 hours they were placed into an electric oven at temperature of 40°C. This cycle was repeated regularly for a year.

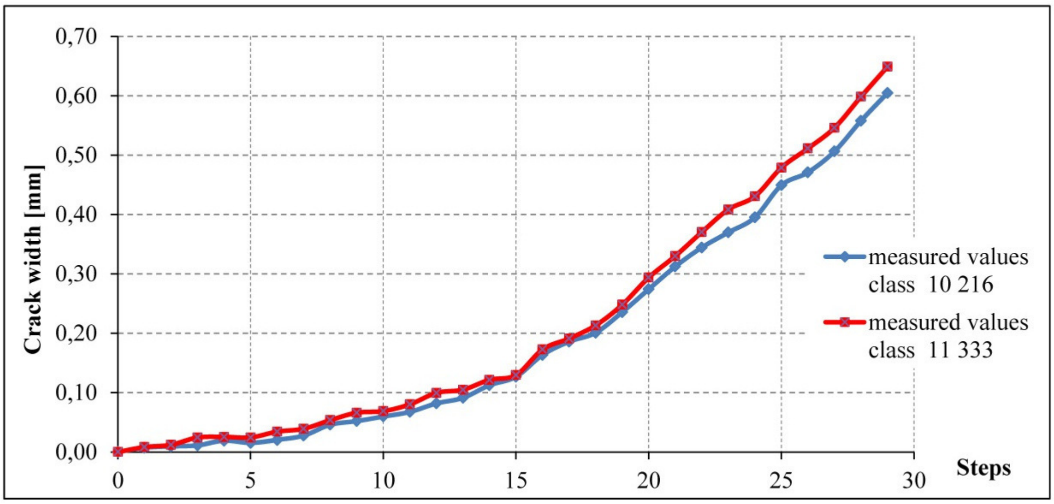

Fig. 2. Experimental results of crack width variation.

3. Numerical modeling of corrosion

The 3D software ATENA was used for numerical modeling of specimens (Fig. 3). Only the specimens (small beams) with smooth-faced reinforcement class 10 216 were modeled. The experiment has confirmed 6 % volume increase of corrosive products during testing period and 7.1 % decrease of bars cross-section. Those data were used as parameters for numerical modeling of initiation, propagation and width of a crack.

The reinforcement cross-section area is decreasing due to corrosion, while the volume of the corrosive products (rust) increase [6, 7]. Due to this phenomenon, it was necessary to recalculate the reinforcement diameter $\phi(t)$ at time t and also the percentage loss of cross-section area of embedded reinforcement (Fig. 3).

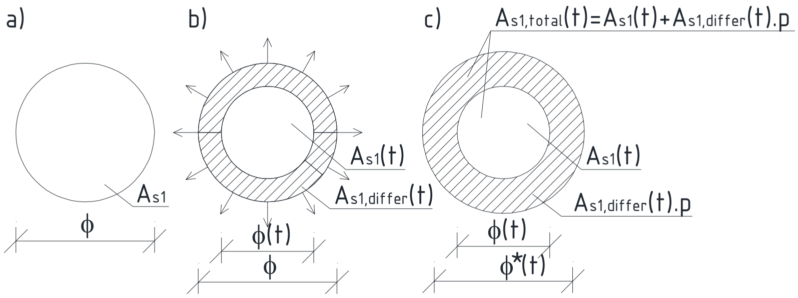

Fig. 3. Change of reinforcement cross-section area due to corrosion – theoretical approach.

The total area of reinforcement at time t is calculated as

$$A_{s1,total}(t) = A_{s1} \cdot (1 + p^*) \tag{1}$$

$$A_{s1,total}(t) = A_{s1}(t) + A_{s1,differ}(t) \cdot (1+p) = \frac{\pi}{4} \cdot \left(\phi^2 \cdot (1+p) - \phi^2(t) \cdot p\right) \tag{2}$$

whereas the experiment has confirmed 6 % increase of corrosion during the testing period, hence follows p = 0.06. The diameter $\phi(t)$ depending on time t was calculated from formula

$$\phi(t) = \sqrt{\frac{\left(-A_{s1,total}(t) + \frac{\pi}{4} \cdot \phi^2 (1+p)\right) \cdot 4}{\pi \cdot p}} \tag{3}$$

Subsequently, the percentage loss of reinforcement cross-section area was calculated

$$p^* = \frac{A_{s1,total}(t)}{A_{s1}} - 1 \tag{4}$$

The corrosion increases non-linearly with time. The model of surface area corrosion was used for calculation of changing of cross-section reinforcement area in single steps. The change of cross-section area is given by formula

$$\phi(t) = \phi - 2 \cdot 0.0116 \cdot (t - t_0) \cdot i_{corr} = \phi - 0.0232 \cdot (t - t_0) \cdot i_{corr} \tag{5}$$

where i_{corr} is the corrosion current density [μA/cm^2], (1 μA/cm^2 is equal to 11.6 μm/year of corroded layer),
t_0 is time of passive stage [8].

The reinforcement volume increasing due to corrosion was put into model as load using shrinkage function, but with the opposite value so as to cause increase of reinforcement volume. This load was evenly distributed within the cross-section and incrementally increases with load steps.

The model of beam was created according to the dimensions of the experiment, with the only difference that the reinforcement does not exceed the concrete part (Fig. 2).

A material "3D Bilinear Steel Von Mises" was used for modeling reinforcement class 10 216 and a material "3D Nonlinear Cementitious 2" was used for modeling concrete elements with strength $f_c = 25$ MN.m^{-2}. The concrete part of specimen was divided into two parts - core and ring with a width of 3 mm. A contact between those two elements was considered as rigid. The reinforcement cross-section was modeled as hexagon with the same cross-section area as original the circle because the 3D version of Atena does not allow to model circular cross-sections. The monitors for cracks width observing were given as global for concrete ring macroelements and for all the three direction of the coordinate system (x,y,z).

The contact between concrete and reinforcement was modeled with material characteristic "3D interface", which is based on Mohr-Coulomb criterion with tension cut off. The constitutive relation for a general three-dimensional case is given in terms of tractions on interface planes and relative sliding and opening displacements and it is given by formula

$$\begin{Bmatrix} \tau_1 \\ \tau_2 \\ \sigma \end{Bmatrix} = \begin{bmatrix} K_{tt} & 0 & 0 \\ 0 & K_{tt} & 0 \\ 0 & 0 & K_{nn} \end{bmatrix} \begin{Bmatrix} \Delta v_1 \\ \Delta v_2 \\ \Delta u \end{Bmatrix} \tag{6}$$

where τ is the shear stress in the x and y directions,
σ is the normal stress,
Δv is the relative displacement on surface,
Δu is the relative opening of contact,
K_{tt} is the initial elastic shear stiffness,
K_{nn} is the initial elastic normal stiffness.

The initial failure surface corresponds to Mohr-Coulomb condition with tension cut off

$$|\tau| \le c + \sigma \cdot ø \quad \mathit{for}\ \sigma \le f_t, \tag{7}$$

$$\tau = 0 \quad \mathit{for}\ \sigma > f_t, \tag{8}$$

where c is the cohesion,
$ø$ is the coefficient of friction,
f_t is the tensile strength on surface.

After stresses violate this condition, the surface collapses into a residual surface, which corresponds to dry friction (Fig. 4).

The cohesion c is equal to surface stresses σ_{surf} and the value $c = 0$ was considered. Also, the coefficient of friction and tensile strength equal to zero were considered ($ø = 0$, $f_t = 0$). The values of initial elastic normal and shear stiffness are estimated from formulae

$$K_{nn} = \frac{E}{t_1},\ K_{tt} = \frac{G}{t_1} \tag{9,10}$$

where E is the minimal elastic modulus,
G is the minimal shear modulus,
t_l is width of the interface zone.

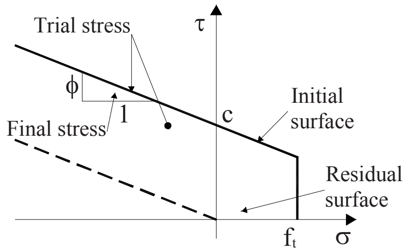

Fig. 4. Failure surface for interface elements in numerical model.

The values $K_{nn} = 3.0 \cdot 10^6$ MN/m^3 and $K_{tt} = 1.0 \cdot 10^{-3}$ MN/m^3 were considered to transfer the compressive stresses from reinforcement to concrete in transverse direction and to ensure the slip between reinforcement and concrete in longitudinal direction. It eliminates the creation on tensile stresses in longitudinal direction.

4. Results of numerical modeling of corrosion

The value p* = 2.488 % was determined from formula (4). This value the best represents the measured values from experiment (curves in Fig. 5). The high consistency of results can be seen in Fig. 5.

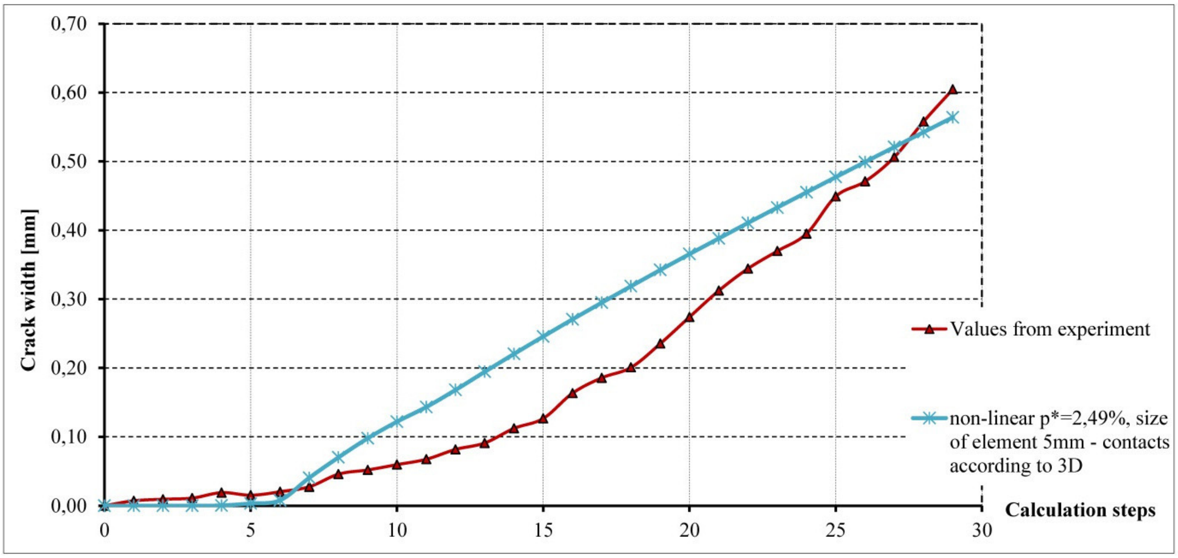

Fig. 5. Comparison of dependency of cracks on numerical models with and without contact.

The cracks propagation in full 3D model is shown in Fig. 6a and crack pattern in the middle cross-section is shown in Fig. 6b and Fig. 6c.

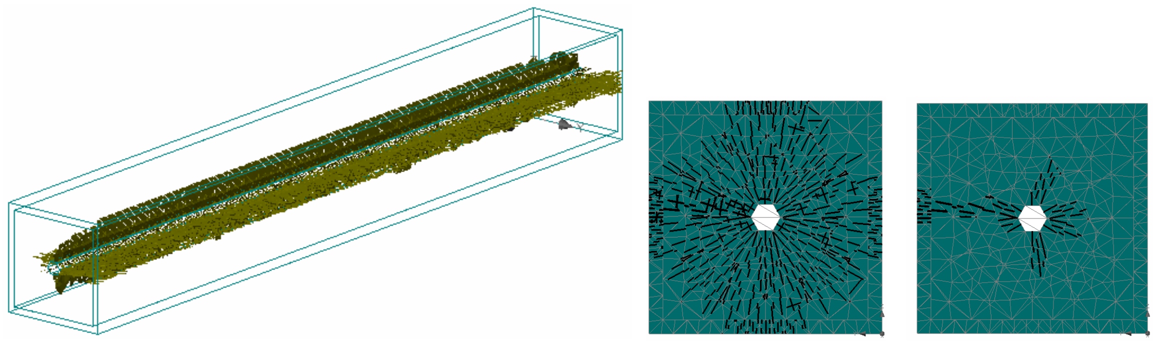

a) full 3D model with cracks b) all cracks c) cracks with width over 0.01 mm (cracks of smaller width were filtered)

Fig. 6. Propagation of cracks from inside towards outside in 3D model.

5. Influence of concrete cover on crack width due to corrosion

The relationship between crack width and the corrosion rate [9] was developed in [10]. The relation has the simple linear format and is given by

$$w = 0.05 + 4.5 \cdot \Delta\phi(t) \tag{11}$$

where $\Delta\phi(t)$ is the thickness of corrosion loss [mm].

Above mentioned dependency was applied to values from experimental measurements (Fig. 9). The results are considerably different. In order to verify and improve the formula, the four small beams (specimens) with various concrete cover were modeled (Fig. 7). Two sides of specimens were doubled in order to more realistically represent the real reinforcement in structures.

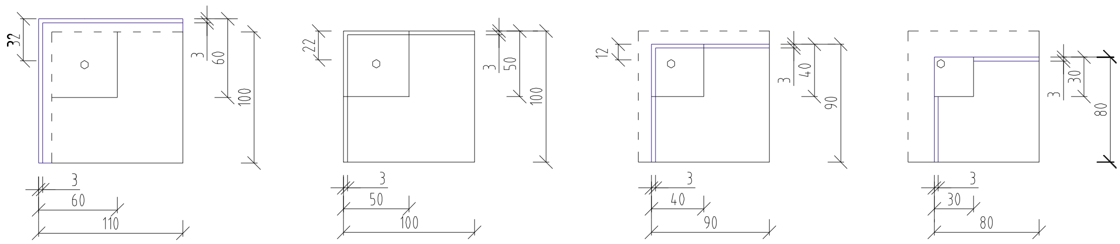

a) concrete cover 32 mm b) concrete cover 22 mm c) concrete cover 12 mm d) concrete cover 2 mm

Fig. 7. Models of specimens with various concrete covers.

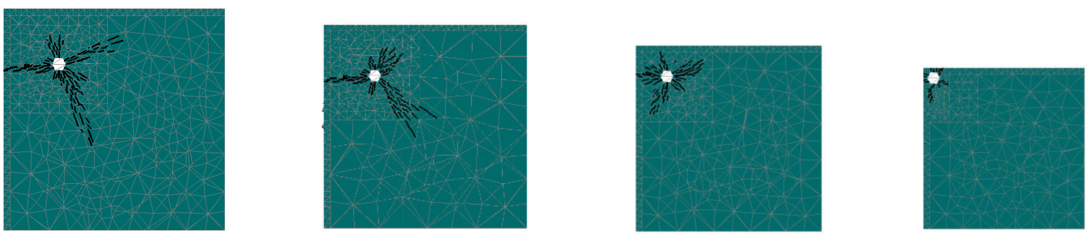

a) concrete cover 32 mm b) concrete cover 22 mm c) concrete cover 12 mm d) concrete cover 2 mm

Fig. 8. Crack development in cross-section of 3D model depending on concrete cover.

The crack development depending on concrete cover dimension shown in the middle of specimens (middle cross-section) is shown in Fig. 8. Just the cracks with crack width over 0.01 mm are shown (the cracks of smaller widths were filtered).

Other factors influence the crack width in structures, as like dimension of concrete cover, the concrete tensile strength and the reinforcement diameter. Those factors are not included in formula (11). For this reason, the formula was modified.

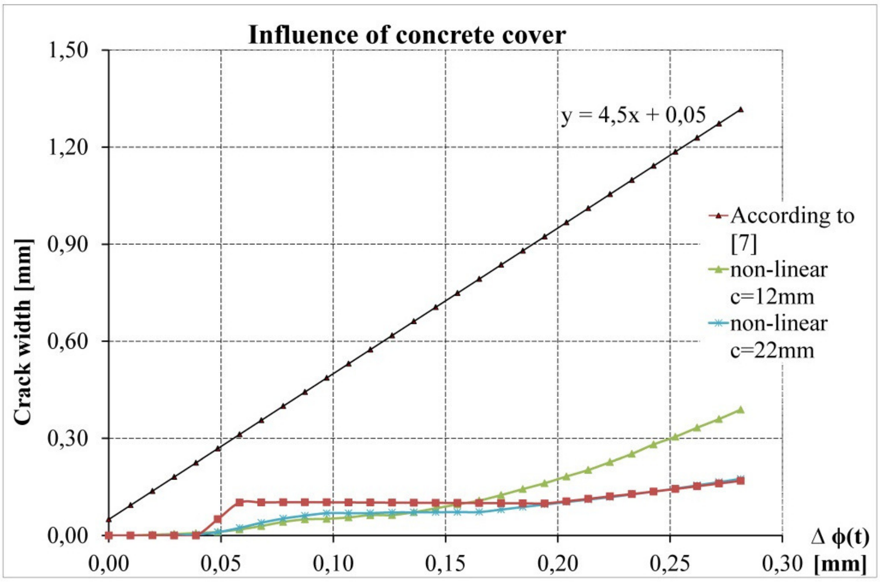

Fig. 9. Influence of concrete cover on crack width.

Since the crack development is not linear, it is best represented by the second degree polynomial. Thus, the quadratic equation was used. The form of formula is influenced by the fact that if the corrosion rate increases so would increase the crack width. Moreover, the crack width is indirectly proportional to the crack length (concrete cover); the longer the crack (concrete cover), the widths smaller.

Base on those considerations, the formula (11) was changed to following form

$$w = \frac{4500}{\phi \cdot c^2 \cdot f_{ct}} \cdot \Delta\phi \tag{12}$$

where ϕ is the reinforcement diameter [mm],
$\Delta\phi$ is loss of thickness due to corrosion [mm],
c is the concrete cover thickness [mm],
f_{ct} is the concrete tensile strength [MN/m^2].

Also the parameter as quality of concrete influences the crack width. The tension strength f_{ct} takes into account that effect.

The curves obtained from numerical modeling were drawn over the curves obtained by application of formula (12). The same values of reinforcement diameter, concrete tension strength and the thickness of corrosion loss were used for all the curves. Only the dimension of concrete cover was changed (Fig. 10).

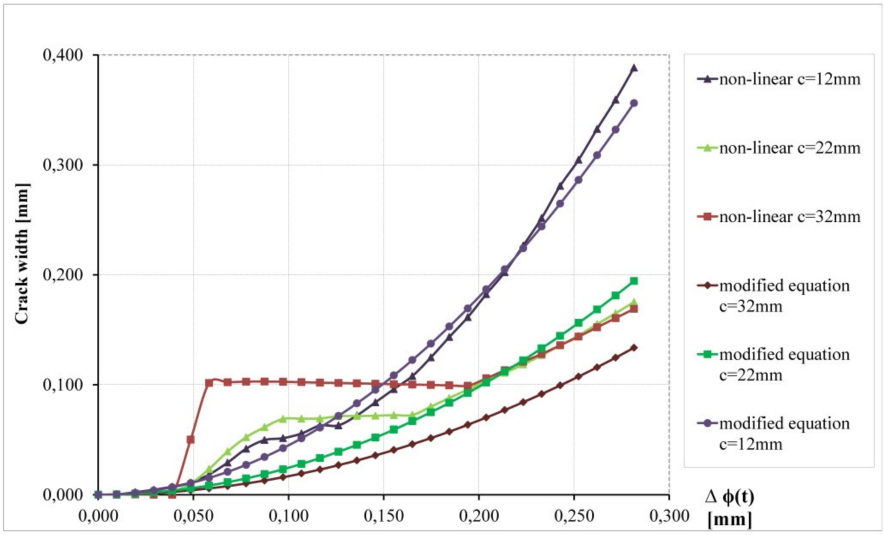

Fig. 10. Influence of concrete cover on crack width.

6. Application on real reinforced concrete girder bridge

The observed bridge is in the village Kolárovice, part of Škoruby, on the road I / 18 over the Kolárovice river (Fig. 11). The reinforced concrete single span girder bridge has a theoretical span of 10.006 m (the length of the bridge is 10.824 m). The width of the road is 7.51 m and the overall width of the bridge is 9.51 m. The bridge skewness is 45.22°. The superstructure consists of a bridge slab having a thickness of 0.19 m and of six main beams with dimensions of 0.325 / 0.84 m. The end diaphragms have dimensions of 0.58 / 0.84 m and three intermediate diaphragms having dimensions of 0.20 / 0.74 m are used to ensure the transverse load distribution.

Fig. 11. Bridge superstructure - view.

The reinforcement corrosion of main girders decreases the remaining lifetime of beams. The corrosion does not only decrease the reinforcement cross-section, but also causes the cracks and dropping out the concrete cover. It means that the flexural stiffness is decreasing. The corrosive reduction rate (rust) causes the pressure at surrounding concrete by increasing its volume. So, the tension stresses are occurring. The micro cracks are created after the concrete tensile strength is exceeded. The micro cracks are connecting into longitudinal cracks by subsequent increasing of corrosive volume reduction rate. The cracks with high corrosive reduction rate are able to cause the decreasing of bond between concrete and reinforcement and following dropping out of concrete cover. The same effect occurs also at some places of spandrel beams (fig.11).

The numerical model of reinforcement corrosion was created in the 3D software ATENA. Only the cross-section of T-girder with real dimensions was modeled (Fig. 12).

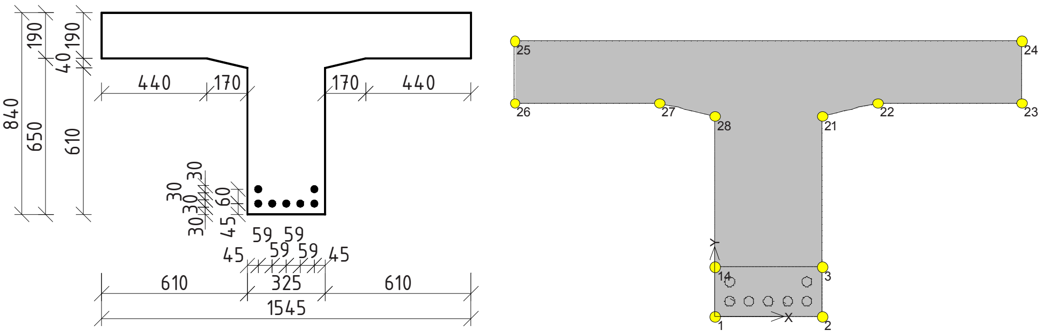

a) The cross-section of T-girder b) The numerical 3D model – cross-section

Fig. 12. Cross-section of T-girder and the numerical model.

The material model of concrete "3D Nonlinear Cementitious 2" with compressive strength $f_c = 40.0$ N.mm^{-2}, was applied for concrete. The basic properties of this material model are: tensile strength, fracture energy and the equivalent uniaxial law. This material model provides objective results due to formulations based on energetical principles and its dependency on the finite element mesh is negligible. The main reinforcement in the RC girder was modelled as the "3D Bilinear Steel von Mises" element with yield strength of $f_y = 210.0$ N.mm^{-2}. Others characteristics are calculated by software ATENA on the basis of redefined formulas. The rigid contacts between concrete and reinforcement were considered.

The initial value of diameter $\phi = 30.0$ mm, the reduced diameter in time $\phi(t) = 28.7$ mm and the percentage $p = 8$ % were considered. So, the final increase of reinforcement area is $p^* = 0.678$ %. This value was used in numerical model. For better monitoring of cracks formation and development, the value p* was divided into ten loading steps. The crack pattern in the cross-section is shown in Fig. 13. It can be seen that the cracks are connected into edge cracks from inside towards the outside (surface) and that was the reason of concrete cover dropping out.

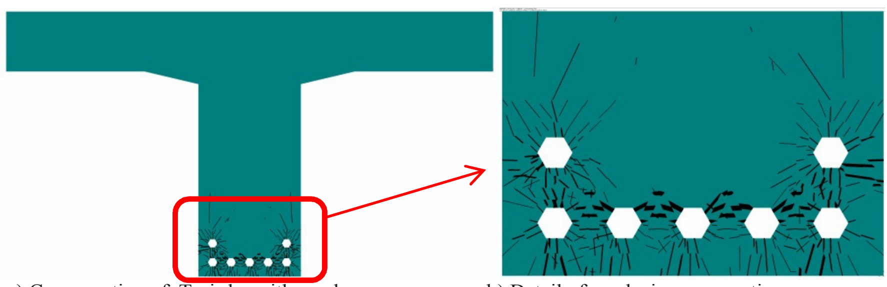

a) Cross-section of T-girder with cracks b) Detail of cracks in cross-section

Fig. 13. Cracks formation and development in loading steps.

7. Conclusions

The results concerning the reinforcement corrosion numerical modeling are presented in the paper. The influence of reinforcement corrosion on the crack formation and propagation were monitored in the cross-section of the specimens in laboratory and in the cross-section of the real reinforced girder of bridge. In the paper was shown that already a small corrosion (percentage of corroded reinforcement area) caused the micro crack formation and propagation inside the cross-section near reinforcement. The micro cracks are connecting into edge cracks due to corrosion increasing which can lead to concrete cover dropping out. In that case, the sufficient strength and bonding of concrete cover is not ensured.

The results from the numerical modeling are compared to experimental measurements. Small differences may be caused by the fact that the cracks width in the numerical modeling was measured globally on the surface (in concrete ring), whereas, the cracks width in the experiment was measured at one place (the crack with maximum width).

Acknowledgements

This work was supported by the Slovak Research and Development Agency under contract No. APVV-0106-11 and by Research Project No. 1/0364/12 of Slovak Grant Agency.

References

[1] STN EN 1990 Basis of structural design, 2009, SUTN.
[2] V. Borzovič, Long-term behaviour composite girders and behaviour under service load, Slovak Journal of Civil Engineering, ISSN 1210-3896, 2006, vol. 14, no. 2, pp. 14-27.
[3] V. Borzovič, J. Halvonik, Flat Slab Reinforcement with Regard to the Distribution and Redistribution of Internal Forces, Third international workshop "Design of concrete structures using Eurocodes", Vienna, Grafische Zentrum HTU GmbH, 2012, pp. 223-228.
[4] K. Gajdošová, Stress and Crack Width Control According to EN 1992, I Third international workshop "Design of concrete structures using Eurocodes", Vienna, Grafische Zentrum HTU GmbH, 2012, pp. 199–202.
[5] J. Vaněrek, Final review of project „Aplication of modern methods for establishing of reinforcement corrosion in reinforced concrete" FRVŠ 1785/2002, VUT FAST Brno, 2002, 10 p.
[6] P. Koteš, M. Brodňan, K. Šlopková, P. Kotula, Numerical modelling of reinforcement corrosion in reinforced concrete, journal "Ochrona przed korozja, "volume 53, 6/2010, pp. 307-309.
[7] P. Koteš, M. Brodňan, K. Šlopková, Simulation of corrosion of reinforcement in reinforced concrete. International RILEM Symposium on Concrete Modelling – CONMOD, 08, CD, Delft – The Netherlands, 2008, [Edited by Erik Schlangen & Geert De Schutter, 2008], pp. 761-766.
[8] P. Koteš, Contribution to determining of reliability level of existing bridge structures, PhD Thesis, Žilina, EDIS 2005, 186 p. (in Slovak).
[9] Fib Bulletin 10, Bond of reinforcement in concrete State-of-art report prepared by Task, Group Bond Models, Sprint-Druck Stuttgard, 2000.
[10] J. Rodriguez, L.M. Ortega, A.M. Garcia, Assessment of structural elements with corroded reinforcemen, Corrosion and Corrosion Protection of Steel in Concrete, Ed. Swamy, R N. Sheffield Academic Press, Sheffield, pp. 171-185.